JOURNAL OF OPTOELECTRONICS AND ADVANCED MATERIALS Vol. 8, No. 4, August 2006, p. 1352 - 1355

Effect of annealing temperature on the electrical and optical properties of nanocrystalline selenium thin films

R. ROY, V. S. CHOUDHARY, M. K. PATRA, A. PANDYA*
Defence Laboratory, Ratanada Palace, Jodhpur- 342 011(Rajasthan) India

Electrical and optical properties of as-grown and annealed films of selenium, grown on glass substrate by thermal evaporation technique at room temperature, have been studied. The as-grown films show variation in resistivity ranging from ~0.44x10^6 to ~3.78x10^6 Ω-cm and the activation energy of ~0.86 eV in temperature range 483 to 573 K. The optical band gap of films has been determined from the transmittance and reflectance spectra taken with the help of spectrophotometer in the wavelength range of 350-900 nm at room temperature. The optical band gap of as-grown films has been found to have direct band gap of ~1.76 eV and a blue shift has been observed for the band gap when their average grain size reduced from ~53 to ~21 nm with increase in annealing temperature, followed by rapid cooling. X-ray diffraction pattern of the films confirmed that all the as-grown films have polycrystalline structure and there is no improvement in crystallinity, rather a reduction in average grain size after annealing.

(Received March 10, 2006; accepted July 20, 2006)

Keywords: Thin films, Selenium, Activation energy, Blue shift, Annealing

1. Introduction

Selenium thin films are very easy to obtain by physical vapour deposition and it should be interesting to use it for cheap large-scale device productions. Growth and characterisation of selenium thin films has been active research subject of considerable interest due to its potential commercial applications in photovoltaic and photoconductive devices. Its low melting point, high vapour pressure and device applications like rectifiers, photocells, switching, memory and X-ray photoconductor etc. [1,2] has made it attractive. Currently, there are many research activities devoted to the development of selenium thin films and their structural and functional properties [3-8]. Their electrical and optical properties are known to strongly depend on film preparation technique, deposition temperature and post-deposition annealing process. It has been shown early [4, 9-11] that the morphological evolution of crystallisation in selenium films, in response to thermal treatment, is quite complicated. Thus we have studied thermal annealing effects, followed by rapid cooling, on the electrical and optical properties of nanocrystalline selenium thin films prepared on glass substrate by thermal evaporation to develop full understanding of this material.

2. Experimental

Thin films were grown by vacuum evaporation of black selenium lumps (99.999%) using molybdenum boat in a high vacuum of 5×10^{-6} mbar on glass substrate kept at room temperature. Prior to deposition, the glass substrates (size: 75×25×1.35 mm^3) were cleaned with acetone and deionised water and dried. The quartz crystal thickness monitor was used for monitoring the film thickness during evaporation. Selenium films of 2 kÅ thickness were deposited at a deposition rate (4-6 Å/s).

The as-grown films were annealed in vacuum (10^{-5} mbar) at two different temperatures, at 398 K and 448 K for 10 minutes, followed by rapid cooling by 10 °C water up to temperature 363 K and then further cooled slowly. Measurements were taken after each annealing cycle. Electrical measurements of the films were done by two-probe method. Ohmic contacts were made on films using high-purity silver paste and fine copper single wires. The ohmic behaviour of the contacts was confirmed by the linear variation of the I-V characteristic, which was independent of the polarity of the applied bias. I-V characteristics measurements were carried on as-grown and annealed films by HP 4145B Semiconductor Parameter Analyser. The temperature dependent d.c. conductivity measurements on as-grown and annealed films between 483 to 573 K were carried out by Keithley Electrometer 6517A.

The optical transmission (%*T*) and reflectance (%*R*) of the films were measured using a double beam UV-VIS-NIR spectrophotometer (Perkin-Elmer Lambda 900) in the wavelength range 350-900 nm, at room temperature. The structural characterisation was carried out by taking XRD pattern of the films with the help of Philips X-ray diffractometer using CuK_α (λ=1.54056 Å) radiations as X-ray source.

3. Results and discussion

Fig. 1 shows the X- ray diffraction studies of selenium film before annealing. X-ray diffraction data of the films

grown at room temperature indicates that they are fine-grained and polycrystalline. X-ray diffraction data of thin films coincides with that of the known trigonal selenium peaks [JCPDS No.: 06-0362]. (100) and (101) reflections (planes) with sharp peaks have been observed in the films. Table 1 shows the 2θ and d-spacing observed along with the standard data (JCPDS No.: 06-0362). The grain size of the prepared films has been calculated using the Scherrer formula. It is found that the average grain size for the most intense peak, (100) reflection is ~53 nm. However, no significant improvement in crystallinity and no additional peak were observed after thermal annealing in vacuum at 398 K for 10 minutes and at 448 K for 10 minutes, followed by rapid cooling. But the films exhibit reduction in the average grain size of the most intense peak, (100) reflection, from ~53 to ~26 nm after first annealing and from ~26 to ~21 nm after the second annealing. Spectroscopic measurements show an increase in the optical bandgap of the films in Fig. 4, further confirms decrease in size. Rapid cooling after annealing leads to the nucleation, and hence reduction in the grain size. Here we note that Byron and Brian [12,13] have devised a solution-phase method for generating nanostructure of selenium in which they have precipitated single crystalline nanoparticles of t-Se in the solution for the growth of t-Se nanowires by quenching the refluxed mixture with ice water. It is clear from the above results as the annealing temperature increases, crystals of selenium tend toward smaller size. Growth occurs in a matter of hours rather than days. The grain size could be controlled by this simple method of thermal annealing followed by rapid cooling.

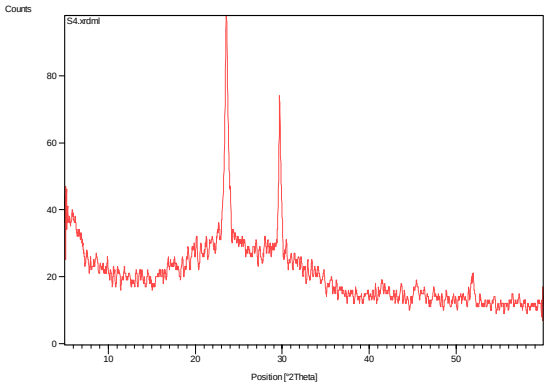

Fig. 1. X-ray diffractogram of the selenium thin film prepared at room temperature, taken with CuK_α radiation.

Table 1. X-ray diffraction data for Se thin film prepared at room temperature.

Standard pattern (JCPDS No.:06-0362)			Prepared film	
(*hkl*)	d (*Å*)	I/I_0(%)	d (*Å*)	I/I_0(%)
(100)	3.780	55	3.78102	100.34
(101)	3.005	100	3.00844	70.14
(201)	1.766	20	1.76231	11.05

Fig. 2 shows the I-V characteristics of as-grown and annealed film. No appreciable change in current values has been observed at lower voltages after annealing of the film at 448 K for 10 minutes in vacuum, followed by rapid cooling. However an increase in current has been observed at higher voltages in annealed film due to high electric field and removal of imperfection by heating [14]. There is little change in conductivity because native defect states compensate any improvement in the films. Native defects in chalcogenides are created from under- and over-coordinated atoms which form charged defects states with a negative electron correlation energy.

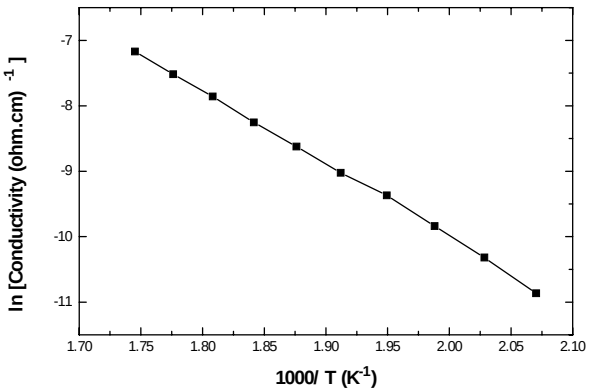

Fig. 2. I-V characteristics of as-grown and annealed selenium film (at 398 K for 10 minutes and then at 448 K for 10 minutes in vacuum, followed by rapid cooling).

Fig. 3 depicts logarithm of conductivity versus temperature plots of as-grown selenium film. It may be noticed that the conductivity increases exponentially with increase in temperature. This shows that the films are semiconducting in nature. Therefore the dc conductivity is given by,

$$\sigma_{dc} = \sigma_0 \exp(-\Delta E_\sigma / k_B T) \quad (1)$$

Where k_B is the Boltzmann constant and σ_0 the pre-exponential factor.

The plots of ln(σ) versus 1000/T is straight line having one slope in the temperature range 483 to 573 K. These plots of the highly resistive selenium samples revealed only one thermally activated process in the high temperature region with activation energy ~0.86 eV determined from the slope of the curve. This temperature region is associated with intrinsic conduction region. Abdul *et al* [3] have reported a value of activation energy of 0.73 eV for low temperature range 250 to 300 K.

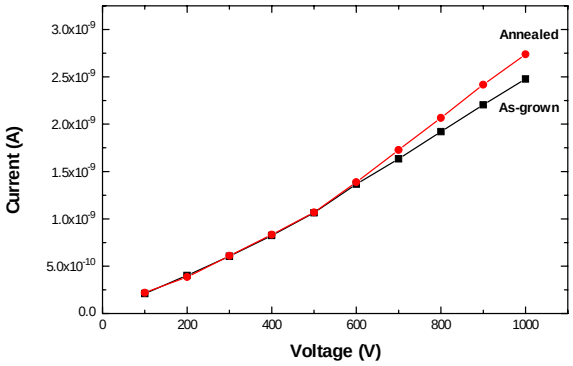

Fig. 3. Variation of ln (σ) vs. 1000/T of a typical as-grown selenium film.

The transmission and reflection data were used to calculate absorption coefficient of the films at different wavelengths. The absorption coefficient, α, is given by the relation [15],

$$T = (1-R)\exp(-\alpha d) \quad (2)$$

Where d is the film thickness.

A sudden decrease at a particular wavelength, in transmission and reflection spectra, indicates the presence of optical band gap in these films. The absorption coefficient data were used to determine energy gap, E_g, using the Tauc relation for direct band gap material [15, 16],

$$\alpha h\nu = A\,(h\nu - E_g)^{1/2} \quad (3)$$

Where constant A, is different for different transitions, ($h\nu$) is the photon energy.

Fig. 4 shows the optical absorption spectra [plots of α^2 versus photon energy $h\nu$ (wavelength range 600-900 nm)] obtained at room temperature of as-grown and annealed selenium films of thickness 2000 Å. It can be seen that the plot is linear in the region of strong absorption near the fundamental absorption edge. Thus, the absorption takes place through direct transition. The values of the direct optical band gap E_g were determined by extrapolating the linear region of the plots to zero absorption ($\alpha h\nu$=0). Optical bandgap of the as-grown films found from the Fig. 4 is ~1.76 eV whereas the reported values by different authors are 1.65 eV for black Se, 1.8 eV for monoclinic and 2.05 eV for amorphous Se by Zienab [8] and 2.09 eV for amorphous Se by Bindu *et al* [5]. The figure shows the thermal annealing effect on the optical absorption spectra of the films. The value of bandgaps of the films come out to be ~1.76, ~1.82 and ~1.84 eV for as-grown, annealed for 10 minutes at 398 K and annealed for 10 minutes at 448 K in vacuum (followed by rapid cooling), respectively. From figure it is observed that with increase in the annealing temperature, keeping the annealing time constant, the slope is decreasing showing the corresponding increase in the bandgap of the film material. The blue shift in bandgap is because of the reduction in grain size from ~53 to ~26 nm and then from ~26 to ~21 nm during the rupturing of Se particles by annealing followed by rapid cooling.

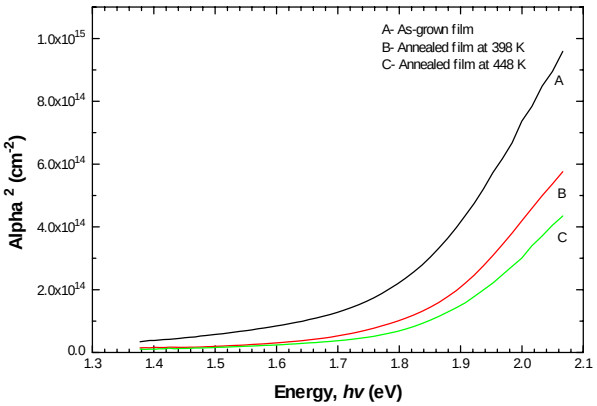

Fig. 4. Plots of α^2 versus photon energy, hv obtained at room temperature of as-grown and annealed selenium films of thickness 2000 Å.

4. Conclusions

Selenium thin films were prepared by thermal evaporation and X-ray studies revealed the formation of nanocrystalline trigonal selenium. Electrical conduction in these films is through a thermal activated process and the activation energy of ~0.86 eV was found in temperature range 483 to 573 K. Electrical properties of the films were not modified by thermal annealing in vacuum due to the defects while spectral measurements suggested a blue-shift in the bandgap with increase in annealing temperature for these selenium films when their average grain size reduced from ~53 to ~21 nm. We could easily change the annealing temperature and other condition to vary the grain size according to our application by this approach. It is reasonable to expect that the availability of cheap high volume production of selenium with low dimensions will introduce new types of application, or enhance the performance of currently existing devices as a result of size confinement.

Acknowledgements

The authors acknowledge Dr. M. P. Chacharkar, Director, Defence Laboratory, Jodhpur for his encouragement and support to this work. The authors also thank Dr. N. Kumar, Head, Camouflage Division and Sri G. L. Baheti, Head, NRMA Division, Defence Laboratory, Jodhpur for their support in carrying out this work.

References

[1] I. Hideo, O. Masayoshi, O. Toshio, T. Akitsu, M. Yoshihiko, Jpn. J. Appl. Phys. **23**, 719 (1984).
[2] A. Tsukamoto, S. Yamada, T. Tomisaki, M. Tanaka, T. Sakaguchi, H. Asahina, M. Nishiki, in: J. T. Dobbins and J. M. Boone (Eds.), Physics of Medical

Imaging, San Diego, U.S.A., Feb 21-27, 1998, SPIE Proc. **3336**, 388 (1998).
[3] M. M. Abdul, G. M. A. Al, B. K. A. Wishah, International J. Electron. **85**, 21 (1998).
[4] K. D. Almeida, K. Napo, G. Safoula, S. O. Djobo, J. C. Bernede, J. Mater. Sci. **35**(12), 2985 (2000).
[5] K. Bindu, M. Lakshmi, S. Bini, C. S. Kartha, K. P. Vijaykumar, T. Abe, Y. Kashiwaba, Semicond. Sci. Technol. **17**, 270 (2002).
[6] A. Legros, M. Shi, A. Mouton, A. Selmani, J. Appl. Phys. **78**(5), 3048 (1995).
[7] X. L. Yuan, S. W. Min, Z. Y. Fang, D. W. Yu, L. Qi, in: S. Zhou, Y. Wang (Eds.), Intl. Conf. on Thin Film Phys. Appli. 1991, SPIE Proc.**1519**, 167 (1991).
[8] S. E., Zienab Mandouh, Fizika A2 1, 35 (1993).
[9] K. S. Kim, D. Turnbull, J. Appl. Phys. **44**, 5237 (1973).
[10] J. P. Audiere, C. Mazieres, J. C. Carballes, J. Non-Crystalline Solids **34**, 37 (1979).
[11] E. A. Chatterjee, S. P. Sen Gupta, J. Mater. Sci. Letters **5**, 559 (1986).
[12] B. Gates, B. Mayers, B. Cattle, Y. Xia, Adv. Funct. Mater. **12**, 219 (2002).
[13] B. Mayers, B. Gates, Y. Xia, Int. J. Nanotechnology **1**, 86 (2004).
[14] M. C. S. Kumar, B. Pradeep, Bull. Mater. Sci. **25**(5), 407 (2002).
[15] H. Kim, C. M. Gilmore, A. Pique, J. S. Horwitz, H. Mattoussi, H. Murata, Z. H. Kafafi, D. B. Chrisey, J. Appl. Phys. **86**(11), 6451 (1999).
[16] J. Tauc, Amorphous and Liquid Semiconductors, Plenum, New-York, 1974, p. 159.

*Corresponding author: arunpandya123@rediffmail.com, b_sahab@yahoo.com